Parametric Mass Modeling for Mars Entry, Descent and Landing System Analysis Study

Jamshid A. Samareh[1] and D. R. Komar [2]
NASA Langley Research Center, Hampton, VA 23681

This paper provides an overview of the parametric mass models used for the Entry, Descent, and Landing Systems Analysis study conducted by NASA in FY2009-2010. The study examined eight unique exploration class architectures that included elements such as a rigid mid-L/D aeroshell, a lifting hypersonic inflatable decelerator, a drag supersonic inflatable decelerator, a lifting supersonic inflatable decelerator implemented with a skirt, and subsonic/supersonic retro-propulsion. Parametric models used in this study relate the component mass to vehicle dimensions and mission key environmental parameters such as maximum deceleration and total heat load. The use of a parametric mass model allows the simultaneous optimization of trajectory and mass sizing parameters.

I. Introduction

MARS design reference architecture 5.0 (DRA5) is the latest NASA study that provides a common framework for future planning of systems concepts and technology development [1]. The Entry, Descent, and Landing (EDL) system is one the critical elements of the entire architecture, and NASA has commissioned a follow on EDL System Analysis (EDL-SA) study to identify and roadmap the EDL technology needed to successfully land large payloads on Mars for both robotic and human-scale missions. The EDL-SA first year results are documented in a NASA report [2], and this paper provides the details of parametric mass models used in the EDL-SA study.

[1] Senior Research Engineer, Vehicle Analysis Branch, MS E401, AIAA Associate Fellow.
[2] Senior Aerospace Engineer, Vehicle Analysis Branch, MS E401.

II. EDL-SA Architecture Set and Mass Models

The EDL-SA exploration class architecture set consists of eight architectures shown in Fig. 1. A detailed discussion on each architecture set can be found in Ref. 1. The architecture set contains five unique components (see

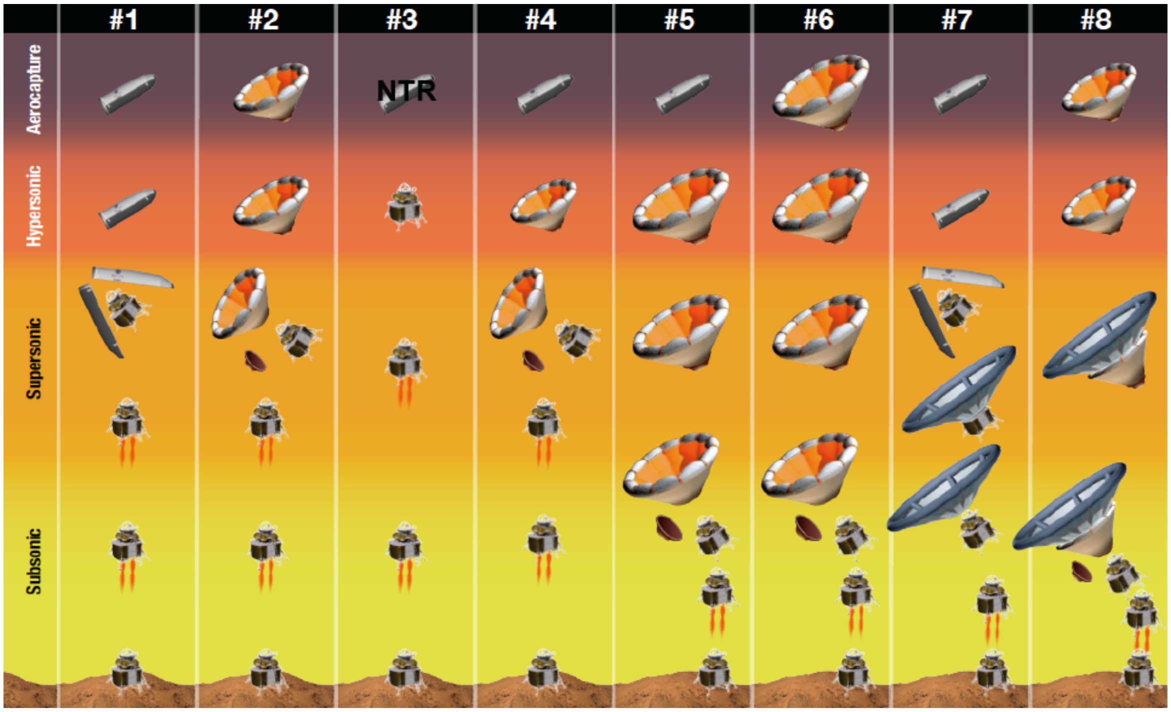

Fig. 1 Exploration class architectures.

Fig. 2): the rigid mid-L/D aeroshell, a lifting hypersonic inflatable decelerator (LHIAD), a drag supersonic inflatable decelerator (DSIAD), a lifting supersonic inflatable decelerator implemented with a skirt on an LHIAD (LSAID–Skirt), and subsonic/supersonic retro-propulsion (SRP). The next section provides an overview of parametric mass models for rigid mid-L/D aeroshell, HIAD, SIAD, and SRP.

III. Parametric Mass Models and Components

There were two key requirements for the EDL-SA mass models: the models had to be parametric and consistent across all architectures. Parametric models are mathematical representations that relate the component mass to the vehicle dimensions and mission key environmental parameters such as maximum deceleration and total heat load. The model consistency is achieved by sharing similar mass model components across all eight architectures.

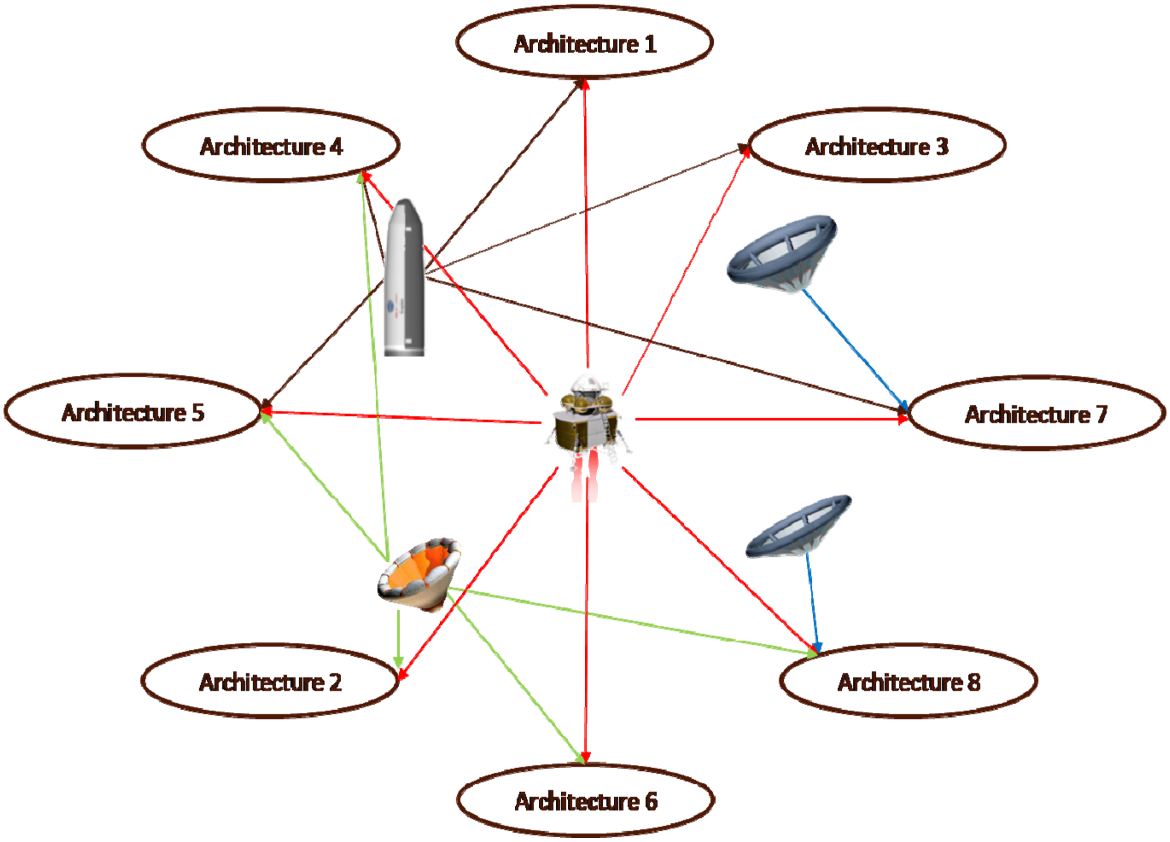

Fig. 2 EDL-SA unique mass components.

A. Rigid Mid-L/D Aeroshell

The rigid mid-L/D aeroshell is a modified version of the dual-use Ares-V shroud used by the DRA5 study [1]. The aeroshell has a straight barrel section with a hemispherical nose cap. The nominal total length is 30 m and the nominal outside diameter is 10 m. (Recent packaging results indicate that a rigid aeroshell with either SRP or SIAD for supersonic deceleration can comfortably fit within the Ares-V shroud; however, simulation results are not yet available for this option.) The mass model for rigid mid-L/D consists of six subcomponents: structure, acoustic blanket, separation mechanism, body flaps, avionics, and TPS.

The Ares-V finite-element (FE) analysis process was used to generate the structural mass estimates. The work was performed by Daniel Pinero and Lloyd Eldred. Loft [3], an in-house computer program, was used to automate the FE model generation with appropriate launch, aerocapture, and entry load cases. NASTRAN® and Hypersizer® were used to analyze and determine optimal structural mass subject to material and buckling constraints that were developed for the Ares-V project. The barrel section consists of eight longerons and six frames (divided into five design groups). The hemispherical nose section consists of 8 longerons formed into one design group. Payload is attached to the second and the fifth frames as shown in Fig. 3. A 25% mass growth allowance was added to the optimal mass to account for minimum gage design, required fasteners, and other structural components not included in the FE model to obtain a current best estimate.

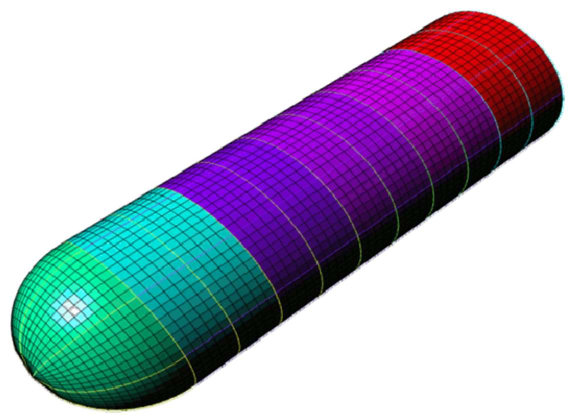

Fig. 3 Finite-element model of the rigid Mid-L/D aeroshell.

A response surface equation (RSE) for the structural mass estimate was developed based on FE mass estimates. The RSE includes the following independent variables: diameter, total length, arrival mass, maximum dynamic pressure, and maximum lateral and axial decelerations. Figure 4 shows structural (structure, acoustic blanket,

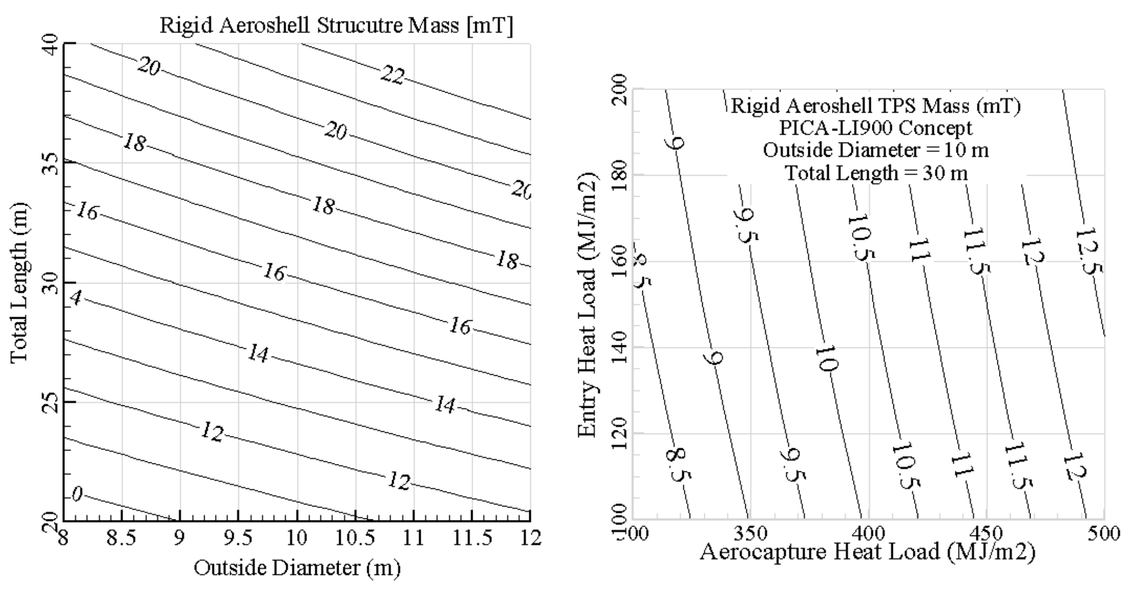

Fig. 4 Structural (left) and TPS (right) mass for the rigid aeroshell of architecture 1.

separation mechanism, body flaps, and avionics) and TPS mass variations for a nominal case, excluding system-level mass growth allowance and system-level margin. The response surface equations for the structure mass model are listed in Table A1 of the Appendix.

Acoustic constraints for the Mars EDL-SA payload are presently unknown. Mars surface power system may include radioisotope systems (RPSs), which could have a considerable impact on the acoustic blanket design. Standard acoustic blankets are most effective at 400 Hz and above (e.g., Titan IV has a 7.62 cm blanket with a one kg/m2 areal density). The Cassini blanket design was driven by radioisotope thermoelectric generators (RTGs) environment, which was qualified for the Galileo and Ulysses missions. The blanket was designed for 200-250 Hz (15.24 cm blanket with a 3.9 kg/m2 areal density). Ares-V is currently (October 2009) using a heavier, 2.54 cm thinner, blanket (15.24 cm blanket with 6.28 kg/m2 areal density), and this blanket is used for the rigid aeroshell model. It is recognized that, depending on the packaging schemes selected for the architectures utilizing IADs, the IAD material may serve a dual use as acoustic blanket. However additional detailed analysis and testing are needed and so for this analysis, the acoustic blanket mass is book kept separately. The mass estimate will be adjusted when there is additional information and a better understanding of Mars EDL payload acoustic requirements and packaging arrangements.

The mass for the body flaps is a point design mass that is added to the aeroshell mass. There are two flaps that are 2 m wide by 13.1 m long; assuming 150 degrees warp angle. The areal density is 16.7 kg/m2 for flaps and 9.8 kg/m2 for the TPS. The mass estimate for flaps includes additional mass for actuation, hydraulics, and APU consumables. However the body flaps were not required in the final analysis.

The TPS is a dual-layer PICA on top of LI-900, and the mass model is function of reference area and total heat load for aerocapture and entry. The TPS mass includes an attachment mass, which is 44% of the TPS mass. Table 1 shows nominal simulation parameters and the mass breakdown for a rigid mid-L/D aeroshell for architecture 1.

Table 1 Nominal parameters and mass breakdown for architecture 1

Variable	Value
Diameter, m	10
Length, m	30
Aerocapture Heat Load, MJ/m^2	345
Entry Heat Load, MJ/m^2	130
Max Dynamic Pressure, kPa	11
Max Lateral Deceleration, m/s^2	29
Max Axial Deceleration, m/s^2	4
Arrival Mass, mT	110

Mass Components	kg
Structure	6341
Acoustic Blanket	6415
Separation System	2065
Avionics	222
Flap	1729
TPS	9199
Total	25971

B. Hypersonic Inflatable Aerodynamic Decelerator (HIAD)

The HIAD design is based on the Mars Inflatable Aeroshell Entry System (MIAS) model [4] that is a 60^o sphere-cone aeroshell. The model consists of an inflatable structure, flexible TPS, avionics, separation system, payload adapter and a rigid payload containment structure known as a heatshield. The inflatable mass model is based on the models developed by NASA in the 1960's and 1970's. The model incorporates a double stacked-toroid consisting of radial straps to tie toroids together and carry radial loads, gores to carry circumference pressure loads, axial straps to carry the buckling loads, torus reinforced fabric to counter the hoop stress, a gas barrier, inflation gas, and gas generators. The straps and reinforcing fabrics are made of Kevlar-49, and the gores and gas barrier are made of Upilex. The mechanical properties of fabrics are reduced for operations in an elevated thermal environment. The design factors of safety for the HIAD follow the NASA standard for soft goods [5].

The toridal structural concept is based on Brown's design [6] that uses a minimum-weight fiber-reinforced film. The design uses widely spaced reinforcing fibers bonded to the surface of the film, as shown in Fig. 5. Brown [6] concludes that the 12X advantage in specific strength of fiber compared to film results in a 7X lower mass, compared to the same size torus fabricated with unreinforced film for the same burst pressure.

It is assumed that the fabric bondline temperature is 200^{o}C with a material knockdown factor of 0.5. The material knockdown factor needs further testing for better understanding. The load factor of safety is set to 4 per NASA requirements for soft goods. Figure 6 shows the HIAD inflatable mass contours for various diameter and maximum dynamic pressures based on a 9 m heatshield diameter. The inflatable mass includes radial straps, gores, tori, inflation gas, and inflation system with appropriate knockdown factors due to an elevated thermal environment, and NASA factors of safety. Solid gas generators are used to produce the inflation gas. The response surface equations for inflatable structure mass model are listed in Table A2 of the Appendix.

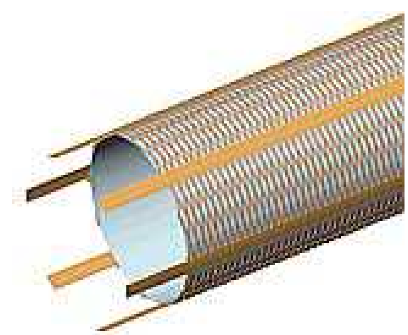

Fig. 5 Reinforcing fibers concept.

Brown [7] recommends using 7.55% of launch mass for the payload adapter. The payload adapter for this study is set to 2% of arrival/entry mass, because the adapter is assumed to carry small mechanical load during launch and it is primarily used during the aerocapture and entry phases.

The flexible TPS is silica felt/silicone, and the parametric model is a function of reference area, the aerocapture heat load, and entry heat load. The current flexible TPS mass model is for an ablator that is limited to diameters less than 50 m. The TPS areal density for aeroshell diameters greater than 50m is held fixed at the areal density of a 50-m aeroshell. The TPS model is suitable for high to moderate heat rates and loads. Due to the large aeroshell diameters, the use of this TPS mass model for architecture 6 may produce less accurate results. The next generation of mass model will include an updated model for a flexible insulator that will be suitable for larger diameters with lower heat rates and heat loads. Figure 6 shows TPS mass contours for architecture 2 as a function of heat loads. Table 2 shows the nominal parameters and mass breakdown for architecture 2.

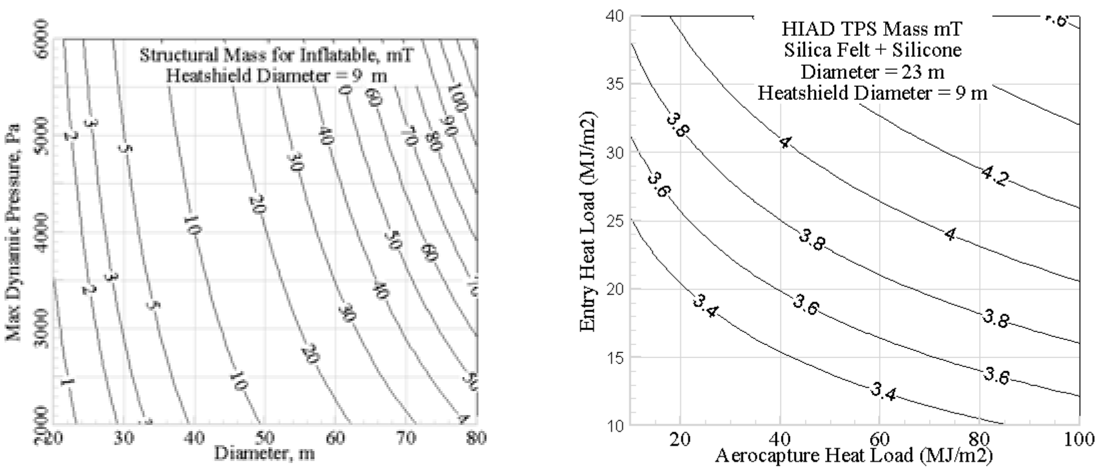

Fig. 6 Inflatable structural (left) and TPS (right) mass for the HIAD of architecture 2.

Table 2 Nominal parameters and mass breakdown for architecture 2

Variable	Value	Components	Mass, mT	%	Areal Density, kg/km^3
Diameter, m	23.0	Adapter	2.2	21.2	5.3
Heatshield diameter, m	9.0	Heatshield	1.1	10.2	2.6
Aerocapture Heat Load, MJ/m^2	87.3	Inflatable	1.8	16.8	4.2
Entry Heat Load, MJ/m^2	26.1	Avionics	0.1	0.9	0.2
Max Dynamic Pressure, Pa	4240.1	Separation	1.3	12.4	3.1
Payload Mass, mT	40.0	TPS	4.0	38.5	9.7
Arrival Mass, mT	83.6	Total	10.5	100.0	25.1
HIAD Mass, mT	10.5				

C. Supersonic Inflatable Aerodynamic Decelerator (SIAD)

The SIAD, deployed after peak heating, is a tension cone model with no TPS and no knockdown factors for fabric due to high temperature. The SIAD model does include NASA recommended factors of safety for loads. A modeling approach similar to HIAD was used to design the SIAD components.

D. Supersonic/Subsonic Retro-Propulsion (SRP)

Architectures 1, 2, and 4 use supersonic RP modules; and architectures 5 through 8 use subsonic RP. Architecture 3 uses RP for the entire EDL segment.

The Exploration Architecture Model for the IN-space and Earth-to-orbit (EXAMINE) [8] modeling tool, developed in-house at NASA Langley, was used to develop the parametric mass estimates of the SRP stage for all architectures.

Three RSE mass models were generated: one for architectures that do not jettison discrete dry mass prior to entry (architectures 1, 2, 6, 7, 8); one for architectures that jettison a portion of the entry system dry mass prior to entry (architectures 4, 5); and one for the all-propulsive architecture (architecture 3). Table 3 shows independent variables as well as the upper and lower limits for the response surface equations. Table 4 shows the dependent variables.

Table 3 SRP independent variables and limits for response surface equations

Architectures	**1,2,4,5,6,7,8**		**3**	
Independent Variable	**Lower Bound**	**Upper Bound**	**Lower Bound**	**Upper Bound**
Payload, mT	10	60	10	60
Terminal Descent ΔV, km/s	0.2	1.5	4	5.5
Initial T/W (Mars g's)	3	11	1	4
Area Ratio	10	200	10	200
Aeroshell (Struc+TPS+misc), mT	5	55	NA	NA
Aerocapture Apo-Correct. ΔV, m/s	0	150	NA	NA
Descent Orbit insertion ΔV, m/s	0	500	NA	NA
Percent pre-entry aeroshell Jettison, %	20*	90*	NA	NA

*Used for architectures 4 and 5

The primary SRP structure is an 8.8 m diameter aluminum-lithium (Al-Li) cylinder that supports the tank system and payload. This primary structural mass is estimated from a historically-based empirical curve fit [9]. Thrust structure mass is based on a historical fit accounting for stage diameter, the number of engines and the thrust load. Secondary structure mass is 25% of the primary plus thrust structure masses. Landing gear mass is 2.5% of the landed mass on Mars. Multilayer insulation (MLI) is 5 cm thick (39.4 kg/m3) covering the exterior structure, providing thermal control of the spacecraft. It is assumed that power is provided by the payload. The design includes a fluid cooling loop that collects heat from the avionics cold-plates and cryogenic tankage (up to 10 kW), and heat is returned to payload thermal cooling system for heat rejection. The avionics model includes UHF, X-band, Ka-band communication systems, quad-fault tolerant flight computer, ranging and Doppler used for interplanetary position determination, and dual-fault tolerant laser radar (LADAR) altimeter for precision landing and hazard avoidance.

Table 4 SRP dependent variables

Dependent Variables
SRP Initial Mass, mT
Aeroshell initial Mass*, mT
Stack Mass at Arrival, mT
Stack Mass at Entry, mT
Stack Mass at Terminal Descent Initiation, mT
Stack Mass at Landing, mT
SRP Propellant Mass, mT
SRP RCS Propellant Mass, mT
Aeroshell RCS propellant mass*, mT
SRP Thrust Per Engine, lbf
Engine T/W (Mars g’s)

*Not Applicable for Architecture 3

Liquid oxygen (LOX) and liquid methane (LCH4) propellants are used for both the main propulsion system (MPS) and the reaction control system (RCS). The MPS has four pump-fed expander engines each operating at 650 psia chamber pressure and a mixture ratio of 3.5. Because stage thrust-to-weight (T/W) and engine area ratio were selected as independent variables, the required thrust varies from case to case and in the overall closure/optimization. Thus, a set of RSE’s for the MPS were developed to quickly predict the engine characteristics (vacuum specific impulse, engine thrust-to-weight, engine length and exit diameter) as a function of required thrust and area ratio. Figure 7 shows the vacuum specific impulse (Ispv) and engine T/W data used in the performance and sizing analysis.

For all architectures except architecture 3, two Al-Li cylindrical LOX tanks and two Al-Li cylindrical LCH4 tanks are packaged within the primary structure with the maximum diameter of each MPS tank limited to 3 m. For the all-propulsive architecture 3, the 2x2 tank packaging arrangement yielded tanks with extremely high length-to-diameters due to the need to package the additional propellant required by the all-propulsive case. At high tank length-to-diameter, the tank and stage structure mass grows quickly and does not allow model convergence. Thus, to limit the maximum tank length-to-diameter, an inline tank arrangement was used for architecture 3 with one forward LOX tank and one aft LCH4 tank, each limited to 8.8 meters in diameter. For all architectures, the MPS tanks stored propellant at 50 psia and utilized advanced cryogenic propellant management technology to minimize boiloff (50 layers of MLI plus single-stage cryocooling system) and provide autogeneous pressurization and control. The RCS has sixteen pressure-fed thrusters each producing 100 lbf. Each thruster operates at a chamber pressure of 125 psia, a mixture ratio of 3.0, and an area ratio of 40, delivering a vacuum specific impulse of 334.5 sec. The RCS propellants are stored at 250 psia in two spherical graphite-wrapped aluminum tanks, one for LOX and one for LCH4. To minimize boiloff, 30 layers of MLI plus a single-stage cryocooling system are employed while a 6000 psia gaseous helium system provides consumables for RCS tank pressurization. For all architectures, 100 m/s ΔV is allocated for RCS operation during landing. For architecture 3, an additional 100 m/s ΔV is allocated for RCS operation during entry.

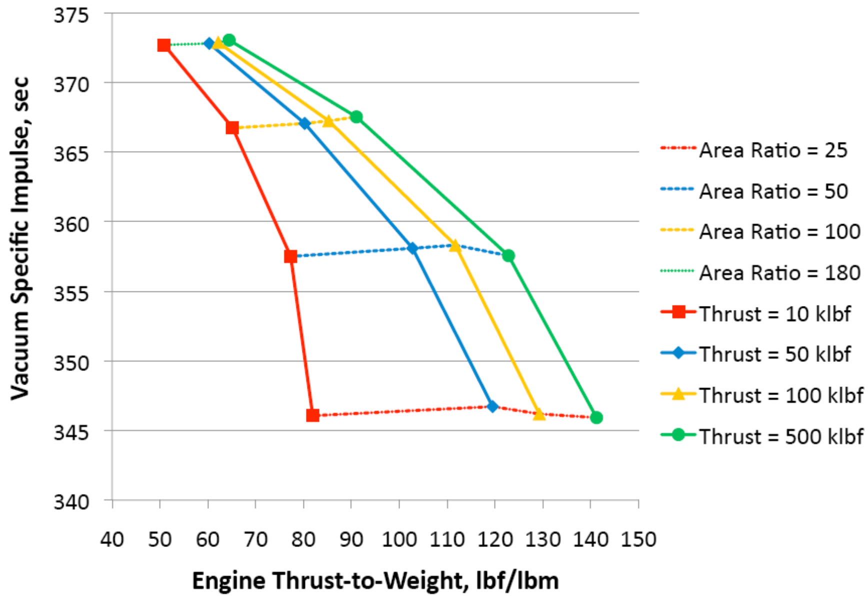

Fig. 7 SRP specific impulse vs. engine thrust-to-weight.

Ground rules of the study required the dry mass growth allowance to be 15% of the basic dry mass and an additional 30% (of the basic mass) is carried as system level margin. Thus, a total of 45% dry mass reserve is included in the mass estimates. Table 5 shows the mass breakdown for architectures 1 and 3. The response surface equations for the descent stage mass model are represented as:

$$y_k = \beta_0^k + \sum_{i=1}^{N} \beta_i^k x_i + \sum_{i=1}^{N} \sum_{j=i}^{N} \beta_{ij}^k x_i x_j$$

where N is the number of independent variables, x_i are the independent variables, y^k are the dependent variables, and β are coefficients for the response surface equations. Values for β for all eight architectures are listed in tables A3-A4 of the Appendix.

Table 5 SRP mass (kg) breakdown for architectures 1 and 3

Mass Item	**Arch 1 - Rigid Mid-L/D Aeroshell**	**Arch 1 - Retro Propulsion Stage**	**Arch 3 - Retro Propulsion Stage**
Primary Body + Thrust Structure	0.0	2076.3	4353.2
Secondary Body Structure	0.0	519.1	1088.3
Aeroshell Structure, TPS, Misc Mass	25111.8	0.0	0.0
Multilayer Insulation	0.0	107.2	83.2
Space Engines & Installation	0.0	1845.9	2623.4
RCS Engines & Installation	202.5	153.7	153.7
MPS Fuel Tanks & Feed/Fill/Drain Sys.	0.0	471.6	1877.4
MPS Oxidizer Tanks & Feed/Fill/Drain Sys.	0.0	512.1	3150.3
RCS Fuel Tanks & Feed/Fill/Drain Sys.	129.9	74.0	267.1
RCS Oxidizer Tanks & Feed/Fill/Drain Sys.	134.4	81.8	310.9
Pressurization System	0.0	90.9	1244.9
Power Management & Distribution	0.0	366.1	366.1
Command, Control, and Data Handling	0.0	12.7	12.7
Guidance & Navigation	0.0	10.3	10.3
Communications	0.0	61.0	61.0
Vehicle Health Management	0.0	0.0	0.0
Cabling and Instrumentation	0.0	35.4	35.4
TCS Heat Acquisition	0.0	120.1	120.1
TCS Heat Transport	0.0	322.9	322.9
TCS Heat Rejection	0.0	325.0	325.0
Landing Legs	0.0	1317.7	1801.6
System Level Margin	7673.6	2551.2	5462.3
Mass Growth Allowance	3836.8	1275.6	2731.1
Dry Mass w/ Growth	**37089.1**	**12330.6**	**26400.9**
Pressurant	2.9	53.2	684.8
Unused Fuel	41.8	73.5	1113.6
Unused Oxidizer	68.9	252.0	3863.4
Inert Mass	**37202.6**	**12709.2**	**32062.8**
Usable OMS Fuel	0.0	3155.8	52258.4
Usable OMS Oxidizer	0.0	11045.3	182904.3
Usable RCS Fuel	2088.9	517.7	3422.1
Usable RCS Oxidizer	3446.7	1553.2	10266.3
Gross Mass	**42738.2**	**28981.2**	**280913.9**

IV. Summary

This paper presented an overview of the parametric mass model used for Entry, Descent, and Landing Systems Analysis study conducted by NASA in FY2009-2010. The paper provides mass models for eight unique exploration class architectures that included elements such as a rigid mid-L/D aeroshell, a lifting hypersonic inflatable decelerator, a drag supersonic inflatable decelerator, a lifting supersonic inflatable decelerator implemented with a skirt, and subsonic/supersonic retro-propulsion.

Acknowledgments

The authors would like to thank Roger Lepsch of Vehicle Analysis Branch (VAB) for providing information on Ares-V acoustic, blanket and Daniel Pinero and Lloyd Eldred of VAB for generating the finite-elements mass estimates for the Mid-L/D aeroshell model.

References

[1] Drake, Bret G., editor, "Human Exploration of Mars Design Reference Architecture 5.0," NASA-SP-2009-566, July 2009.

[2] Dwyer-Cianciolo, A. M., et al., "Entry, Descent and Landing Systems Analysis Study: Phase 1 Report," NASA–TM–2010–216720, July 2010..

[3] Eldred, L. B., "HSLoad - Input Deck Documentation", NASA LaRC SAMS Contract No. NAS1-00135 03RAA, Swales Aerospace Corporation. 5/28/2003.

[4] MIAS Design Reference Report, Astrium GmbH, MIAS-RIBPRE-RP-0002, Dec. 4, 2002.

[5] Structural Design and Test Factors of Safety for Spaceflight Hardware, NASA-STD-5001A, August 5, 2008

[6] Brown, G. J., "Inflatable Structures for Deployable Aerocapture Decelerators," Proceedings of JANNAF Conference, 2005.

[7] Brown, C. D., Elements of Spacecraft Design, American Institute of Aeronautics & Astronautics, April 2003.

[8] Komar, D. R., Hoffman, J., and Olds, A., "Framework for the Parametric System Modeling of Space Exploration Architectures," AIAA-2008-7845, 2008.

[9] Heinemann, W., "Design Mass Properties II: Mass Estimating and Forecasting for Aerospace Vehicles Based on Historical Data," JSC-26098, November 1994.

Appendix

Table A1 Response surface equations for rigid aeroshell structure mass

	Lower Bound	Upper Bound	Variable Names	Sample Result	Mass Model Equations
Aerocapture Mass Minus Strucuture Mass, mT	100	150	C1	110	
Diameter, m	8	12	C2	10	
Barrel Length, m	25	35	C3	25	
Max Aerocapture and Entry Dynamic pressure, kPa	0	20	C4	11	
erocapture and Entry Lateral Deceleration, Earth Gs	0	4.5	C5	3.0	
Max Aerocapture and Entry Axial Deceleration, Earth Gs	0	-2	C6	-0.4	
Total Surface Area, m2			C7	1021	PI()*C2*(C3+C2/2+C2/4)
Structural Mass, kg			C8	5073	C7*EXP(-1.5774462 + LN(C1) * (0.58278956) + LN(C2) * (-0.8533078) + LN(C3) * (0.65239167) + C4 * (-0.00765) + C5 * (0.133) + C6 * (0.00748))
Total Structural Mass, kg			C9	6341	C8*1.25
Smeared Unit Mass, kg/m2			C10	6.21	C9/C7

Table A2 Response surface equations for HIAD aeroshell structure mass

	Lower Bound	Upper Bound	Variable Names	Sample Result	Mass Model Equations
	HIAD Mass Model I				
HIAD Diameter, m	20	80	d	24	
Max Dynamic Pressure, Pa	100	2000	q	2000	
Approximate HIAD Mass, kg			Mass	1093	Mass = PI()/4 * d * d * (0.19820998 + d *(0.01535624) + q *(-0.0003258) + d*d *(-0.0001801) + d*q *(0.0000540113) + q*q *(0.00000000286428))
	HIAD Mass Model II				
HIAD Diameter, m	20	80	d	40	
Max Dynamic Pressure, Pa	2000	6000	q	3600	
Approximate HIAD Mass, kg			Mass	9005	Mass = PI()/4 * d * d * (0.19820998 + d * (0.01535624) + q * (-0.0003258) + d*d * (-0.0001801) + d* q * (0.0000540113) + q* q * (0.00000000286428))

Table 3 Response surface equations for SRP With pre-entry Jettison (architectures 4 and 5)

	β for y_1	β for y_2	β for y_3	β for y_4	β for y_5	β for y_6	β for y_7	β for y_8	β for y_9	β for y_{10}	Coefficients
β_0	14326.39978	3635.524434	16523.59663	15025.02987	14326.41801	7892.969223	6003.343639	430.1051469	3027.626343	54147.42272	1
β_1	-91.47900323	-65.36388636	870.3488775	944.9254405	908.5217152	978.7667228	-97.52048327	27.27547566	-61.86729418	-1005.416806	x1
β_2	-11.05228284	-5.07654094	-15.02557746	-11.51881789	-11.0523177	-2.617218021	-8.103288984	-0.331810696	-4.776826855	-50.14870646	x2
β_3	-1121.148657	-345.2086858	-1396.624959	-1167.721729	-1121.156217	-646.3587027	-441.1383641	-33.65915047	-324.6894458	-8026.923499	x3
β_4	-22.52470712	-6.50388667	-27.73998312	-23.45430636	-22.5248152	-6.986992866	-14.86158638	-0.676235954	-6.116428336	-62.59135307	x4
β_5	-15.27081291	1601.768824	1586.211931	1493.941116	-15.26986036	-10.95607017	-3.855361189	-0.458429004	142.4310293	-25.17681323	x5
β_6	-3.277783843	-6.296040341	2.320512205	-1.937874964	-3.277887265	-2.575698719	-0.603780403	-0.098408142	-6.009463446	-4.860339261	x6
β_7	-0.983335153	-3.446033222	-3.372793678	-0.229097543	-0.983366181	-0.772709617	-0.181134121	-0.029522443	-3.295962046	-1.45810178	x7
β_8	-12.93059416	41.1406261	29.39594412	-12.6992174	-12.93021976	-9.591573802	-2.950457221	-0.388188734	38.70758066	-20.55531683	x8
β_{12}	0.558896297	0.095290643	0.637762033	0.581821038	0.558895255	0.074642208	0.467473993	0.016779053	0.08961322	0.82445268	x1*x2
β_{13}	25.80284272	4.399174979	29.44389533	26.86131411	25.80296214	19.43097904	5.597331213	0.774651892	4.137211617	370.8283059	x1*x3
β_{14}	0.489920143	0.083533608	0.559054567	0.510015728	0.489917465	0.430811319	0.044397932	0.014708214	0.078552752	0.758059358	x1*x4
β_{15}	2.47E-12	-0.002383421	-0.002460802	-0.001462477	1.10E-11	1.02E-11	4.60E-13	3.30E-13	-1.14E-04	2.27E-11	x1*x5
β_{16}	-3.23E-12	0.672810146	0.040075491	0.014429423	-3.86E-12	-1.89E-12	-1.85E-12	-1.16E-13	0.63290095	-5.07E-12	x1*x6
β_{17}	1.16E-13	0.673693349	0.656795954	0.024995805	1.07E-12	1.01E-12	3.08E-14	3.21E-14	0.633667103	1.47E-12	x1*x7
β_{18}	-1.53E-11	0.032856743	-0.010061215	-0.113565205	-2.28E-11	-1.38E-11	-8.34E-12	-6.86E-13	0.03003373	-4.63E-11	x1*x8
β_{23}	0.775580152	0.132285433	0.885084765	0.807426596	0.775592089	0.343357717	0.408949685	0.023284686	0.124361312	5.970329481	x2*x3
β_{24}	0.010690753	0.00182328	0.012200029	0.011129634	0.010690917	0.006849799	0.003520157	3.21E-04	0.001714172	0.016872535	x2*x4
β_{25}	5.10E-13	-3.02E-05	-3.62E-05	-3.36E-05	1.07E-12	7.87E-13	2.52E-13	3.21E-14	1.70E-06	1.92E-12	x2*x5
β_{26}	8.45E-15	0.009768501	5.82E-04	2.10E-04	5.88E-14	5.03E-14	6.74E-15	1.76E-15	0.009189023	1.35E-14	x2*x6
β_{27}	-6.36E-14	0.009781273	0.009535937	3.63E-04	-1.24E-13	-9.09E-14	-2.92E-14	-3.72E-15	0.009200178	-2.39E-13	x2*x7
β_{28}	-1.06E-13	4.77E-04	-1.46E-04	-0.001648291	-1.64E-13	-9.55E-14	-6.32E-14	-4.93E-15	4.36E-04	-1.73E-13	x2*x8
β_{34}	4.000740788	0.682586108	4.565759491	4.165043906	4.000749921	3.060056658	0.820583468	0.120109795	0.641509761	9.909985317	x3*x4
β_{35}	1.15E-10	-0.001340024	-0.001754255	-0.001956789	2.57E-10	1.87E-10	6.21E-11	7.72E-12	1.60E-04	2.84E-10	x3*x5
β_{36}	1.57E-12	0.474264769	0.028258578	0.010175263	1.53E-11	1.43E-11	4.77E-13	4.58E-13	0.446120671	-4.55E-12	x3*x6
β_{37}	1.94E-12	0.474878851	0.462966654	0.017617297	1.06E-11	1.00E-11	2.86E-13	3.19E-13	0.446670561	5.82E-12	x3*x7
β_{38}	-1.53E-11	0.02316597	-0.007074118	-0.080003481	-1.57E-11	-7.24E-12	-7.94E-12	-4.73E-13	0.021159724	-3.90E-11	x3*x8
β_{45}	-2.30E-12	1.29E-05	-4.17E-05	-1.57E-04	-4.32E-12	-2.92E-12	-1.27E-12	-1.30E-13	3.57E-05	-5.53E-12	x4*x5
β_{46}	-6.98E-13	0.008200889	4.89E-04	1.76E-04	-1.00E-12	-5.64E-13	-4.08E-13	-3.01E-14	0.007713821	-2.09E-12	x4*x6
β_{47}	-4.58E-13	0.008211284	0.008005338	3.05E-04	-8.97E-13	-6.22E-13	-2.49E-13	-2.69E-14	0.007723647	-1.28E-12	x4*x7
β_{48}	-3.82E-12	4.01E-04	-1.22E-04	-0.001383123	-6.79E-12	-4.52E-12	-2.07E-12	-2.04E-13	3.65E-04	-1.07E-11	x4*x8
β_{56}	2.38E-12	0.321965236	-0.20947808	0.007806966	6.51E-12	5.22E-12	1.09E-12	1.95E-13	0.302713489	8.61E-12	x5*x6
β_{57}	4.96E-13	0.273449705	0.268976235	0.010051805	1.49E-12	1.27E-12	1.80E-13	4.48E-14	0.257234263	2.48E-12	x5*x7
β_{58}	0.063105292	-1.996183026	-1.90182481	-15.06927225	0.063081203	0.030610087	0.030577304	0.001893813	-1.876329445	0.139628943	x5*x8
β_{67}	-1.04E-12	0.011513897	-2.59E-04	2.12E-04	-6.25E-13	5.73E-14	-6.64E-13	-1.88E-14	0.010905196	-2.88E-12	x6*x7
β_{68}	-1.58E-11	-0.003130864	0.016985758	-0.015718927	-2.57E-11	-1.66E-11	-8.34E-12	-7.73E-13	-0.0024615	-4.04E-11	x6*x8
β_{78}	7.93E-14	-0.186631443	-0.184980459	-0.02195591	5.79E-12	5.86E-12	-2.35E-13	1.74E-13	-0.175526017	4.47E-14	x7*x8
β_{11}	-0.311525714	-0.058215928	-0.35817152	-0.325703178	-0.311529104	-0.231774822	-0.070401612	-0.009352671	-0.052444393	-0.451481165	x1**2
β_{22}	0.004794405	8.11E-04	0.005467871	0.004990646	0.004794388	4.43E-04	0.004207109	1.44E-04	7.62E-04	0.007016409	x2**2
β_{33}	18.66152483	3.070137244	21.27746612	19.41858015	18.66113841	14.30038656	3.800510505	0.560241344	2.884686004	260.6656332	x3**2
β_{44}	-0.056085302	-0.009710917	-0.063988092	-0.058404094	-0.056086302	-0.080756295	0.026353806	-0.001683813	-0.009128705	-0.081730388	x4**2
β_{55}	0.196667031	0.030221248	0.223528598	0.204261614	0.196673236	0.154541923	0.036226824	0.005904489	0.028905516	0.291620356	x5**2
β_{66}	0.021851892	0.01185087	0.025393343	0.023027816	0.021852582	0.017171325	0.004025203	6.56E-04	0.01118909	0.032402262	x6**2
β_{77}	0.00196667	0.006696746	0.008469414	0.002276897	0.001966732	0.001545419	3.62E-04	5.90E-05	0.006331478	0.002916204	x7**2
β_{88}	0.100340322	0.019122779	0.117658079	0.13060475	0.100343488	0.07884792	0.018483074	0.003012494	0.018060152	0.148785896	x8**2

x1 Payload, mT
x2 Terminal Descent DV, km/s
x3 Initial T/W (Mars g's)
x4 Area Ratio
x5 Aeroshell (Struc+TPS+misc), mT
x6 Aerocapture Apo-Correct. DV, m/s
x7 Descent Orbit insertion DV, m/s
x8 Percent pre-entry aeroshell Jettison, %
y1 SRP Initial Mass, mT
y2 Aeroshell initial Mass, mT
y3 Stack Mass at Arrival, mT
y4 Stack Mass at Entry, mT
y5 Stack Mass at Terminal Descent Initiation, mT
y6 Stack Mass at Landing, mT
y7 SRP Propellant Mass, mT
y8 SRP RCS Propellant Mass, mT
y9 Aeroshell RCS propellant mass*, mT
y10 SRP Thrust Per Engine, lbf

Table 4 Response surface equations for SRP with no pre-entry jettison (architectures 1, 2, 6, 7, and 8)

	β for y_1	β for y_2	β for y_3	β for y_4	β for y_5	β for y_6	β for y_7	β for y_8	β for y_9	β for y_{10}	Coefficients
β_0	18142.37359	9548.287668	25691.98155	19757.30454	18142.30486	10559.40564	7038.234201	544.6650161	8590.715089	64315.7846	1
β_1	-130.7168504	-85.83753313	813.7455383	894.3086465	869.2857488	951.2567788	-108.0685705	26.09754053	-81.10229915	-1079.738884	x1
β_2	-12.60424068	-5.94664471	-17.32434578	-13.40125096	-12.60421055	-3.850249404	-8.375559801	-0.378401344	-5.59553548	-53.26361099	x2
β_3	-1378.494491	-546.7676062	-1831.684548	-1459.539892	-1378.484961	-839.6074291	-497.4929045	-41.38462778	-514.2756377	-8431.261175	x3
β_4	-32.38618099	-19.03408054	-49.20181161	-34.67059065	-32.3859752	-13.02517851	-18.38851076	-0.972285927	-17.90322773	-110.9493566	x4
β_5	-38.32795655	1479.209742	1454.015808	1462.530005	-38.32834401	-28.96692434	-8.21073301	-1.150686656	27.01716997	-59.63900604	x5
β_6	-11.02482642	-19.9648475	-15.9653731	-12.54185261	-11.02478719	-8.230057136	-2.463745873	-0.33098418	-18.86513703	-17.38762432	x6
β_7	-9.92472471	-17.65462597	-25.47330393	-11.28805742	-9.924763261	-6.377743219	-3.249060583	-0.297959459	-16.66695054	-32.28468959	x7
β_{12}	0.560947888	0.100296558	0.644629127	0.586437781	0.56094655	0.075128321	0.468977593	0.016840637	0.09431911	0.830518555	x1*x2
β_{13}	26.00705727	4.732422807	29.96713988	27.19381804	26.00706076	19.51139035	5.71489111	0.780779304	4.450542883	371.8767176	x1*x3
β_{14}	0.479789289	0.120391906	0.585101168	0.503716384	0.479789325	0.429773745	0.035611431	0.014404149	0.113226066	0.760404659	x1*x4
β_{15}	5.14867E-07	0.086318987	0.007460234	0.002376233	1.34403E-06	9.45712E-07	3.57966E-07	4.03502E-08	0.084023209	2.43743E-06	x1*x5
β_{16}	3.81E-06	0.680435233	0.04562799	0.041730268	8.39E-06	5.90E-06	2.24E-06	2.52E-07	6.40E-01	1.52E-05	x1*x6
β_{17}	4.88E-02	0.68841707	0.71869651	0.092742708	4.88E-02	2.40E-02	2.33E-02	1.47E-03	0.64756466	1.06E-01	x1*x7
β_{23}	7.80E-01	0.153247422	0.909537515	0.816042279	7.80E-01	3.45E-01	4.11E-01	2.34E-02	0.144090714	5.99E+00	x2*x3
β_{24}	1.00E-02	0.003596685	0.013252095	0.010562379	1.00E-02	6.78E-03	2.91E-03	3.00E-04	0.003382743	1.64E-02	x2*x4
β_{25}	4.40087E-07	0.001489595	0.000126833	5.13783E-05	9.67701E-07	6.80483E-07	2.58166E-07	2.90522E-08	0.001440894	1.75495E-06	x2*x5
β_{26}	6.6008E-09	0.009890343	0.000663406	0.000606536	1.7231E-08	1.21244E-08	4.58927E-09	5.17E-10	0.009304007	3.12489E-08	x2*x6
β_{27}	2.45E-03	1.03E-02	1.24E-02	3.16E-03	2.45E-03	1.87E-03	5.00E-04	7.35E-05	9.69E-03	6.04E-03	x2*x7
β_{34}	3.99E+00	1.756881892	5.60E+00	4.24E+00	3.99E+00	3.05E+00	8.25E-01	1.20E-01	1.652270479	9.80E+00	x3*x4
β_{35}	7.15E-05	0.077598343	0.006670309	2.95E-03	1.57E-04	1.11E-04	4.20E-05	4.72E-06	0.074902367	2.85E-04	x3*x5
β_{36}	1.07E-06	4.82E-01	3.23E-02	0.029560887	2.80E-06	1.97E-06	7.46E-07	8.41E-08	4.53E-01	5.08E-06	x3*x6
β_{37}	0.156354937	0.508189912	0.647852358	0.192935061	0.156361156	0.106260964	0.045405946	0.004694247	0.478035956	0.255812288	x3*x7
β_{45}	3.01E-06	0.003642476	0.000274406	0.00019795	6.62E-06	4.66E-06	1.77E-06	1.99E-07	3.46E-03	1.20E-05	x4*x5
β_{46}	4.52E-08	0.00811763	0.000547362	0.000498596	1.18E-07	8.30E-08	3.14E-08	3.54E-09	0.007635745	2.14E-07	x4*x6
β_{47}	2.00E-02	0.011510902	0.030765969	0.021444741	2.00E-02	8.68E-03	1.08E-02	6.02E-04	0.010827766	1.64E-01	x4*x7
β_{56}	4.13E-02	0.660801106	0.123032602	0.082296518	4.13E-02	2.01E-02	2.00E-02	1.24E-03	0.622503884	8.96E-02	x5*x6
β_{57}	5.15E-08	6.23E-01	6.02E-01	3.83E-02	1.34E-07	9.46E-08	3.58E-08	4.03E-09	5.86E-01	2.44E-07	x5*x7
β_{67}	3.81E-07	0.022191582	6.25E-03	1.28E-03	8.39E-07	5.90E-07	2.24E-07	2.52E-08	0.020956506	1.52E-06	x6*x7
β_{11}	7.90E-02	0.036213731	0.093437963	8.24E-02	7.90E-02	7.14E-02	5.25E-03	2.37E-03	0.035518198	1.39E-01	x1**2
β_{22}	5.37E-03	9.52E-04	6.14E-03	0.005615945	5.37E-03	8.92E-04	4.32E-03	1.61E-04	8.95E-04	7.89E-03	x2**2
β_{33}	3.39E+01	6.745954306	38.90494643	35.50517421	3.39E+01	2.61E+01	6.76E+00	1.02E+00	6.337442802	2.84E+02	x3**2
β_{44}	-2.90E-02	-0.00323879	-0.032778939	-0.030235933	-2.90E-02	-5.98E-02	3.16E-02	-8.72E-04	-0.003051182	-4.09E-02	x4**2
β_{55}	0.587197393	0.123199539	0.673709664	0.613818434	0.587184624	0.457682731	0.111873542	0.017628351	0.116991761	0.881865986	x5**2
β_{66}	6.52E-02	0.022616986	7.56E-02	6.89E-02	6.52E-02	5.09E-02	1.24E-02	1.96E-03	0.021288866	9.80E-02	x6**2
β_{77}	5.87E-03	0.010001916	0.01528723	0.006648482	5.87E-03	4.58E-03	1.12E-03	1.76E-04	0.009446522	8.82E-03	x7**2

x1 Payload, mT
x2 Terminal Descent DV, km/s
x3 Initial T/W (Mars g's)
x4 Area Ratio
x5 Aeroshell (Struc+TPS+misc), mT
x6 Aerocapture Apo-Correct. DV, m/s
x7 Descent Orbit insertion DV, m/s
y1 SRP Initial Mass, mT
y2 Aeroshell initial Mass, mT
y3 Stack Mass at Arrival, mT
y4 Stack Mass at Entry, mT
y5 Stack Mass at Terminal Descent Initiation, mT
y6 Stack Mass at Landing, mT
y7 SRP Propellant Mass, mT
y8 SRP RCS Propellant Mass, mT
y9 Aeroshell RCS propellant mass*, mT
y10 SRP Thrust Per Engine, lbf

Table 5 Response Surface Equations for SRP (Architecture 3)

	β for y_1	β for y_2	β for y_3	β for y_4	β for y_5	β for y_6	β for y_7	β for y_8	Coefficients
β_0	1373241.82	1373241.82	979550.934	950143.032	160462.781	1136492.54	76286.5041	1088582	1
β_1	-11309.973	-10309.974	-7357.6358	-7136.7462	-154.13496	-9582.8335	-573.00575	-9271.9059	x1
β_2	-521.84104	-521.84102	-372.81903	-361.62632	-55.3194	-437.48682	-29.034795	-350.96773	x2
β_3	-108195.43	-108195.46	-77045.934	-74732.874	-18405.188	-83790.003	-6000.2647	-211594.36	x3
β_4	-552.90593	-552.90639	-374.47104	-363.22874	-103.12895	-420.61399	-29.163452	-325.40307	x4
β_{12}	3.37505131	3.37505146	2.39233525	2.32051299	0.30137036	2.88736828	0.18631282	1.81588855	x1*x2
β_{13}	494.831751	494.831786	350.927209	340.391735	113.229254	354.272651	27.3298805	1712.72325	x1*x3
β_{14}	-0.1844684	-0.1844657	0.30008179	0.29107279	0.56607315	-0.773909	0.02337009	0.08518313	x1*x4
β_{23}	20.6364528	20.6364599	14.6362042	14.1967987	3.30313578	16.1934703	1.1398538	40.6453649	x2*x3
β_{24}	0.00614561	0.00614569	0.01323087	0.01283365	0.01293845	-0.0078232	0.00103041	0.01061096	x2*x4
β_{34}	64.9719601	64.9719353	47.6298593	46.1999243	17.0250906	44.2374761	3.70936859	32.5104101	x3*x4
β_{11}	-0.9364	-0.9364015	-0.5515218	-0.5349641	-0.1017269	-0.7917227	-0.042952	-0.2283031	x1**2
β_{22}	0.05211069	0.05211068	0.03715393	0.0360385	0.00511208	0.04410509	0.00289351	0.02750291	x2**2
β_{33}	1550.3426	1550.34021	1131.19647	1097.23589	400.844277	1061.39942	88.0965157	5129.53617	x3**2
β_{44}	1.45795605	1.45795621	0.78169781	0.75822982	0.00408032	1.39299799	0.06087789	0.77942814	x4**2

x1	Payload, mT
x2	Terminal Descent DV, km/s
x3	Initial T/W (Mars g's)
x4	Area Ratio
y1	SRP Initial Mass, mT
y2	Stack Mass at Arrival, mT
y3	Stack Mass at Entry, mT
y4	Stack Mass at Terminal Descent Initiation, mT
y5	Stack Mass at Landing, mT
y6	SRP Propellant Mass, mT
y7	SRP RCS Propellant Mass, mT
y8	SRP Thrust Per Engine, lbf